Reprint from: The Roots of Modern Biochemistry
Editors: Kleinkauf, von Döhren, Jaenicke
© 1988 Walter de Gruyter & Co., Berlin · New York

Architecture of Ribosomal Particles as Investigated by Image Reconstruction and X-Ray Crystallographic Studies

H.G. Wittmann and A. Yonath

Introduction

Ribosomes are cell organelles on which the biosynthesis of proteins occurs, and they are present in all organisms. The best studied ribosomes are those of bacteria, especially of Escherichia coli and Bacillus stearothermophilus. The ribosomal particles of these organisms contain approximately 55 proteins and three (5S, 16S and 23S) RNA chains. The primary structures of the RNAs and most of the proteins have been determined (1–3).

Furthermore, a battery of chemical, physical and immunological methods, especially immune electron microscopy, neutron scattering and cross-linking, have been used for the investigation of the ribosomal architecture, i.e. the spatial arrangement of the proteins and RNAs within the ribosomal particles (4, 5). The results of these studies have already given a first insight into the architecture of the bacterial ribosome, although a model at the molecular level is still lacking. As a step towards obtaining such a model we have undertaken diffraction studies on two-dimensional crystalline arrays and on three-dimensional single crystals of ribosomes and their subunits.

Image Reconstruction Studies on Crystalline Arrays

Three-dimensional image reconstruction permits the determination of the surface of the objects from periodically ordered two-dimensional arrays. This is useful for the elucidation of structures of large biological macromolecules and assemblies at moderate resolution. In spite of some inherent limitations, image reconstruction has grown in popularity and is now considered a standard procedure. It involves averaging, by Fourier transformation, of images obtained by electron microscopy of tilt series of periodically organized identical objects. We have performed three-dimensional image reconstruction studies on two-dimensional ordered arrays of 50S subunits and of 70S ribosomes from *Bacillus stearothermophilus.*

50S ribosomal subunits

The two-dimensional arrays of 50S ribosomal subunits have at first been grown in vitro from low molecular weight alcohols by vapor diffusion in hanging drops (AL sheets). Recently, mixtures of salts and alcohols have been used for the growth of

the arrays in depression slides or on electron microscopy grids (ST sheets). The two-dimensional arrays of 50S particles consist of small unit cells: 145×350 Å, $\gamma = 89°$ for the alcohol-grown arrays, and 148×370 Å, $\gamma = 109°$ for those grown from salts. For both (ST) and (AL) arrays each unit cell contains two particles with dimensions similar to those obtained by other methods, e.g. electron microscopy. The arrays are well ordered, and optical diffraction patterns of electron micrographs of negatively stained specimens with gold-thioglucose extend to 28–30 Å.

Images of the arrays were recorded at a minimum dose of the specimens tilted at angles up to 60°, at intervals of 5°, with respect to the incident electron beam. For Fourier transforms, optical densities of arrays (512×512) were used, and reciprocal lattices were fitted to the calculated diffraction patterns. Amplitudes and phases were extracted from peaks of at least two-standard deviations above background (6).

Based on the molecular weight of the 50S ribosomal particle (1.6×10^6) and on the thickness of the sheets observed by image reconstruction (160–170 Å), the calculated density of a 50S particle is 1.3–1.4 g/cm^3, and the V_m for a hypothetical crystal is 2.6–2.7 Å^3/Da. Both values are in good agreement with the average values tabulated by Mathews (7) and those calculated for other large nucleoprotein structures.

Interparticle contacts within the arrays are clearly revealed in the resulting three-dimensional map. The best defined contact area is of 5–12 Å diameter, compatible with the regular intermolecular contacts found in crystals of proteins or nucleic acids. Since details as small as these are beyond the resolution of our map, we cannot yet identify the exact nature of these contacts.

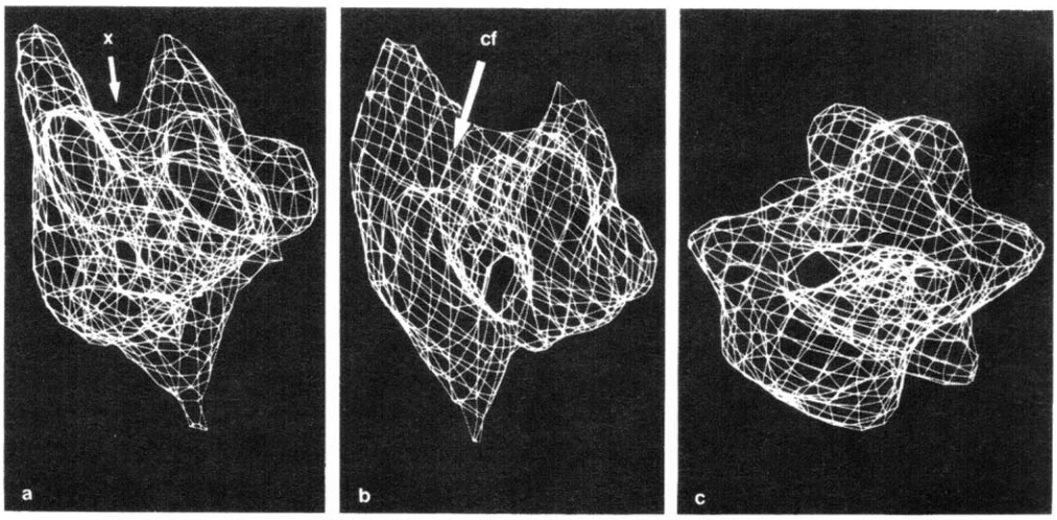

Figure 1 Computer graphic display of the reconstructed model of the *Bacillus stearothermophilus* ribosomal 50S subunit. (a) A side view of the model. (b) The model shown in (a) rotated arround the X axis, showing the cleft (cf) between the projecting arms, at the site where it turns into the tunnel. (c) A view into the tunnel from the cleft. More details are described in reference (6).

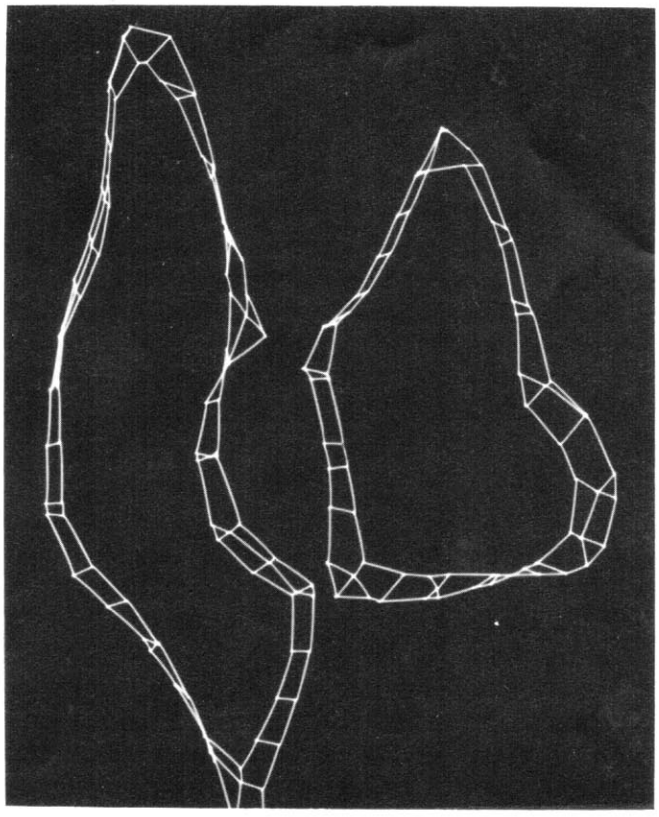

Figure 2 Outline of a 20 Å thick section in the middle of the reconstructed 50S model (Figure 1), showing that the tunnel spans the particle.

Several striking features have been revealed in the resulting model. The concave surface of the particle consists of several protrusions of 25–30 Å diameter, which is the approximate size of globular proteins of molecular weights typical of many ribosomal proteins. Several projecting arms, two of which are longer than the others, are arranged radially around the edge near the interface with the 30S subunit. A narrow elongated cleft is formed between the projecting arms, and turns into a tunnel of a maximal diameter of 25 Å and 100–120 Å length (Figure 1). This tunnel is clearly seen in Figure 2 where a section through the reconstructed model of the 50S particle is shown.

Thirteen reconstructed particles were studied. The tunnel is present in all reconstructions of the arrays independent of the staining material. Furthermore, indications of such a tunnel are detected in some filtered images of particular tilts (6). In every reconstructed particle there is also a region of low density which branches off the tunnel to form a Y (or V) shape, and terminates on the opposite side of the particle (Figure 1). As yet the exact nature of this region cannot be determined. It may be a loosely packed protein region, but in some reconstructed models the density of this region is so low that it appears as a branch of the main tunnel.

Three-dimensional image reconstruction was also applied to two-dimensional arrays of 50S ribosomal subunits stained with uranyl acetate instead of gold-thioglucose described above. Although the arrays were large and well orderd, the diffraction patterns of their micrographs extended only to 32 Å and were of lower quality than those from gold-thioglucose. This might stem from the fact that uranyl acetate, in contrast to gold-thioglucose, is not a pure negative stain and may interact with selected parts of the particle (presumably the rRNA). This interaction may depend on the accessibility to the stain and therefore be somewhat irregular. Consequently, the reconstructed model shows somewhat less details. The essential features, namely the concave shape, the tunnel and the projecting arms, are nevertheless resolved. Comparison of this model with that obtained from the arrays stained with gold-thioglucose shows two regions (on one of the long arms and on the body of the particle), where uranyl acetate, acting as a positive stain, is incorporated into the particle. This may indicate that in these regions the rRNA is concentrated and/or easily exposed to the stain.

Several models for the 50S ribosomal subunits from *E. coli* have been suggested previously, based on electron microscopical visualization, reconstruction or averaging of single particles (4, 5). Our model is more similar to those having no flat surfaces and to those in which the projecting arms are arranged radially around one side of the particle. On the other hand, our model can be positioned so that its projected view (Figure 3) resembles the usual image seen when single particles are investigated by electron microscopy. In addition, there are a few filtered images of two-dimensional arrays tilted by certain angles, which show the same shape and include the characteristic features that have been visualized by electron microscopy of single particles (6).

However, there are also some discrepancies in the nature of the gross structural features between our model and the others. These probably stem from the basic differences between visualization of isolated particles in projection by electron

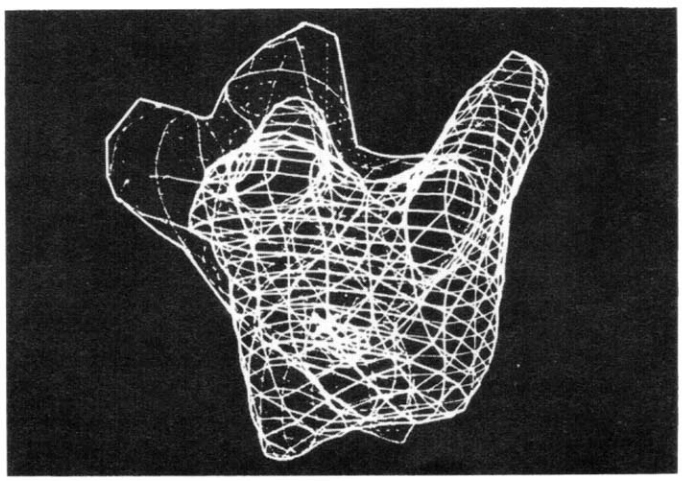

Figure 3 The reconstructed model (Figure 1) viewed in a projection which resembles models derived from electron microscopy of single 50S particles.

microscopy and the subjective interpretation of the pictures on the one hand, and the inherently much more objective character of structure analysis by diffraction methods on the other hand. There are a few preferred orientations in which the isolated particles tend to lie on grids. As a result of the contact with the flat grids, their projected views are likely to be somewhat distorted, and their surfaces may appear flat rather than curved. In contrast, particles within the crystalline arrays are held together by interparticle contacts. These contacts construct a network which may stabilize the conformation of the particles and decrease, or even eliminate, the influence of the flatness of the grids. Thus, the particles within ordered arrays provide a more suitable starting point for reconstruction studies.

The functional significance of the tunnel is still to be determined. However, since it originates at the site for protein biosynthesis and terminates at the other end of the particle, as well as being of a diameter large enough to accommodate even the largest amino acids, the tunnel appears to provide the path taken by the nascent polypeptide chain. Furthermore, this tunnel is of a length which could accommodate and protect from proteolytic enzymes a peptide of about 40 amino acids, as has been postulated from biochemical studies (8–10). It remains to be seen whether the tunnel terminates at a location compatible with that assigned by immune electron microscopy as the exit site for the growing polypeptide chain (11). A narrow elongated region of low density has also been revealed on ribosomes from lizards by three-dimensional image reconstruction (12).

70S ribosomal particle

The two-dimensional arrays of 70S ribosomal particles from *Bacillus stearothermophilus* (Figure 4) consist of relatively small unit cells: $(190 \pm 15) \times (420 \pm 15)$ Å, $\gamma = 107° \pm 3°$. Optical diffraction patterns of electron micrographs of negatively stained specimens with uranyl acetate extended to 40 Å. Attempts to stain the arrays with gold-thioglucose resulted in their destruction. Therefore, they were cross-linked with about 1% glutaraldehyde prior to staining. This procedure caused some loss of internal order, and negatively (with gold-thioglucose) stained cross-linked arrays diffracted to 47 Å resolution (13).

The model obtained by three-dimensional image reconstruction of the ribosomal 70S particle (Figure 5) has average dimensions similar to those determined by other physical methods. The reconstructed volume (2.8×10^6 Å^3) corresponds to about 90% of the whole particle. Several interesting features are revealed by the analysis of the gold-thioglucose stained arrays. The two ribosomal subunits are arranged around an empty space with a volume of up to 4×10^5 ($\pm 2 \times 10^5$) Å^3.

There are some variations in the size of this space as revealed in different reconstructions. This may result from ribosomes which may carry some components, such as tRNA, elongation factors or fractions of mRNA, in variable amounts. Since no attempts were made to remove the nascent polypeptide chain from the ribosome, the tunnel which provides the path for this chain (Figure 2) may be, at least partially, filled. In fact, compared to the 50S particles, here the tunnel is

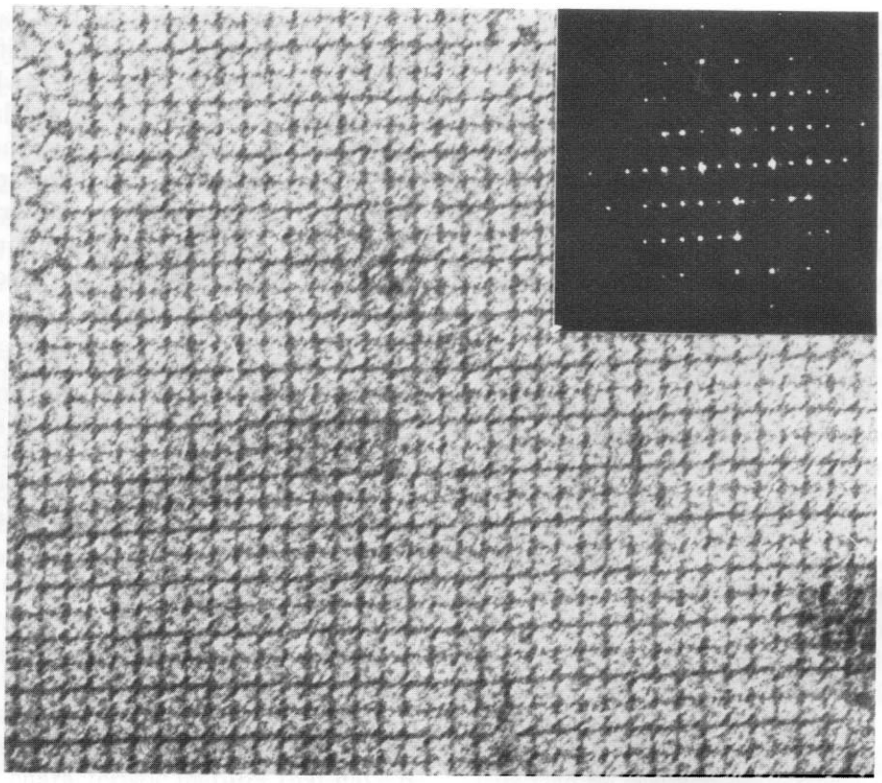

Figure 4 Electron micrograph of a two-dimensional array of 70S ribosomes from *Bacillus stearothermophilus*. An optical diffraction pattern is inserted.

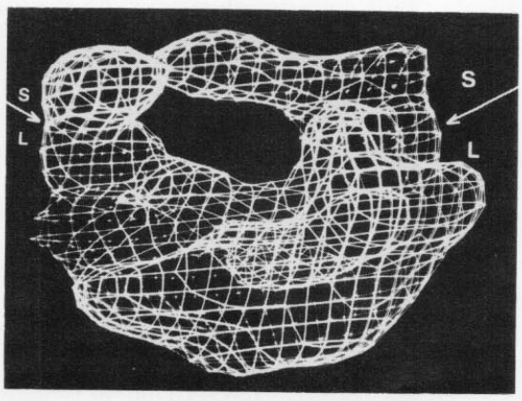

Figure 5 Computer graphic display of the reconstructed model of 70S ribosomes stained with gold-thioglucose. The small and large ribosomal subunits are marked by S and L, respectively.

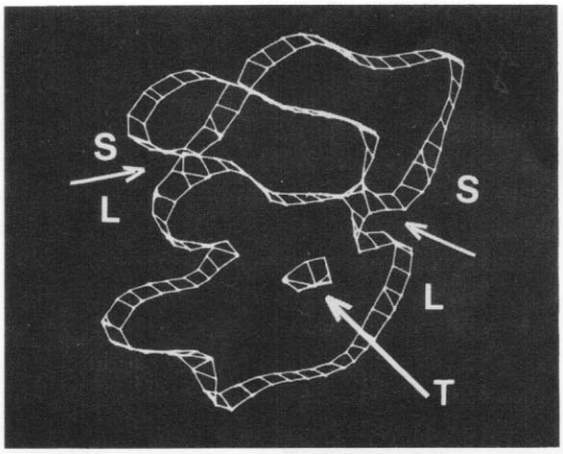

Figure 6 Outline of a 20 Å thick section in the middle of the reconstructed 70S model (Figure 5). T: part of the tunnel.

only partially resolved, and evidence for its existence is obtained by investigating sections through reconstructed particles (Figure 6).

The two ribosomal subunits are fairly well separated. Only the two ends of the small subunit are in contact with the large one. The overall shapes of both subunits have been compared with models which have previously been suggested for these particles (4, 5). There is a good agreement between the 50S particle as seen in Figure 1 and the one within the 70S ribosome (Figure 5). In general, there is also a similarity between the model of the small subunit obtained by visualization of single particles and that revealed by our studies. However, isolated 30S particles seem to be shorter than the reconstructed ones within the 70S particles. As discussed above for the 50S ribosomal subunit, this may be a consequence of the contact of the isolated particles with the flat electron microscope grids, whereas particles within the crystalline arrays are held together by their interactions with the neighboring particles as well as by interparticle crystalline forces. In this way the conformation of the particles is conserved, and the influence of the flat grid is decreased.

We have also reconstructed models from ribosomal arrays stained with uranyl acetate instead of with gold-thioglucose (13). The arrays used for these studies were large and well ordered. As mentioned above, uranyl acetate, in contrast to gold-thioglucose, functions also as a positive stain, since it may interact with selected portions of the object. In the case of ribosomes the extent of interaction of uranyl acetate depends on the accessibility of RNA. As seen in Figure 7, regions which were stained by uranyl acetate are located on the large subunit in its surface area which faces the internal empty space. Furthermore, penetration of uranyl acetate to the region assigned as "collar's ridge" on the small subunit was also observed. In both cases the staining of these areas with uranyl acetate may stem either from the existence of exposed ribosomal rRNA regions and/or from the presence of mRNA and tRNA in these locations.

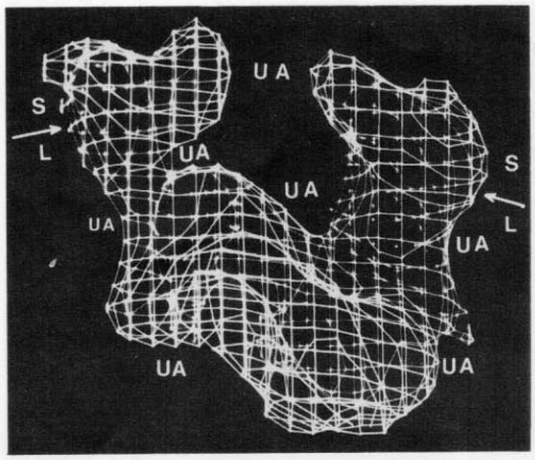

Figure 7 Computer graphic display of the reconstructed model of 70S ribosomes stained with uranyl acetate. Areas of substantial interaction with the stain are marked by UA.

X-Ray Crystallographic Studies

The best method for the determination of the spatial structure of biological macromolecules is X-ray crystallography. This technique has advanced rapidly, especially in collecting, processing and analyzing crystallographic data. Synchrotron radiation provides the most intense, intrinsically parallel X-ray beam, and it is essential for crystallographic data collection from single crystals of ribosomal particles because of their large unit cell dimensions.

Three-dimensional crystals have been obtained from 70S ribosomes as well as from 30S and 50S ribosomal subunits of various bacteria, and in all cases only biologically active ribosomal particles could be crystallized. The best crystals for X-ray structure analysis obtained so far are those of the 50S subunits from the thermophilic *Bacillus stearothermophilus* (14) and from the extremely halophilic *Halobacterium marismortui* (15).

50S Ribosomal Particles from *Bacillus stearothermophilus*

Because ribosomes from eubacteria, to which *Bacillus stearothermophilus* belongs, disintegrate at high salt concentrations, volatile organic solvents had to be used as precipitants. A modified version of the standard hanging drop technique, using glass plates, was developed (16). The crystallization droplets, which contained either no precipitant or an extremely small quantity of it, were equilibrated with a reservoir containing the precipitant. Attempts to increase the size of these crystals by a drastic slow-down of the crystallization process failed, since ribosomal particles from this

bacterium are unstable and may deteriorate before they are able to aggregate and form proper nucleation centers.

Growing crystals from volatile organic solvents imposes many technical difficulties in manipulating, data collection and heavy-atom derivatization. In fact, any handling of the crystals, such as removing or reorienting the crystals, or replacing the growth medium by a different solution, is extremely difficult. Thus, for this system seeding was virtually impossible. However, reducing the size of the exposed

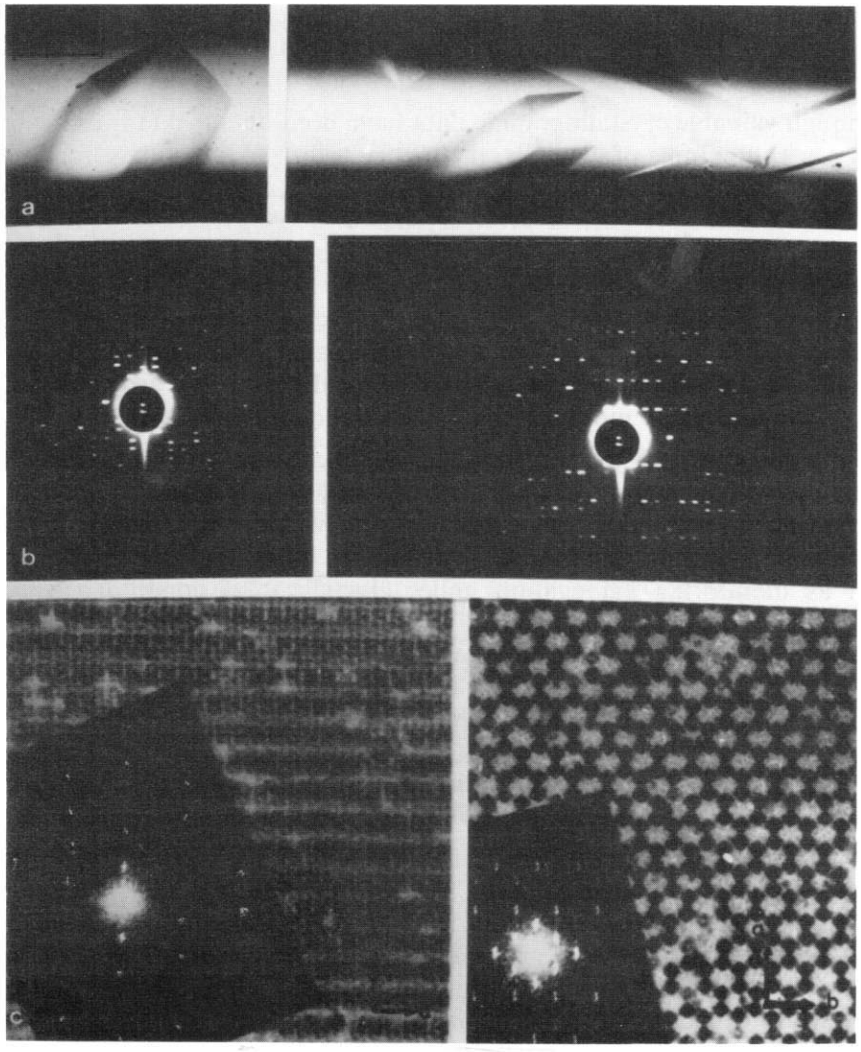

Figure 8 (a) Crystals of ribosomal 50S particles from *Bacillus stearothermophilus*. (b) X-ray diffraction patterns of the major zones obtained with synchrotron radiation. (c) Electron micrographs of thin sections through the crystals. The section on the right shows the open packing of this crystal form, and is approximately perpendicular to that on the left. Optical diffraction patterns are inserted. For details see ref. (17).

surface of the crystallizing droplet led to the production of large crystals (16). This was achieved by growing crystals directly in X-ray capillaries.

Crystals from the 50S subunits of *Bacillus stearothermophilus*, which may reach a length of 2.0 mm and a cross-section of 0.4 mm, are obtained at 4 °C from mixtures of methanol and ethylene glycol. Since most of the crystals grow with one of their faces adhering to the walls of the capillaries, it is possible to irradiate them without removing the original growth solution. Although many crystals grow with their long axes parallel to the capillary axis, a fair number grow in different directions. Thus, we could determine the unit cell constants and obtain diffraction patterns from all of the zones without manipulating the crystals. The crystals are loosely packed (Figure 8) in a unit cell of $360 \times 680 \times 920$ Å. They diffract to 13–18 Å resolution. They often last a few hours in the synchrotron beam, but the higher resolution terms are lost within 5–10 minutes.

Although valuable crystallographic data have been obtained (14) from the crystals grown with mixtures of alcohols, there were technical difficulties in manipulating, data collection and heavy-atom derivatization. Therefore, we searched for an alternative, and were able to grow crystals of 50S subunits from *Bacillus stearothermophilus* ribosomes using polyethylene glycol. The particles in these crystals, in contrast to those grown from alcohols, are tightly packed. Crystallographic measurements show that the new crystals diffract to better than 14 Å, and periodic spacings of 260 Å, 320 Å and 700 Å were calculated from their diffraction patterns. Since these crystals can be much better handled than those grown from alcohols, they are considerably more suitable for crystallographic studies.

The process of crystal growth is initiated by nucleation. Although many biological molecules and complexes have been crystallized, currently little is known about the mechanism of nucleation. Most of the data available concerning the process of nucleation of crystals of biological systems are based on rather indirect evidence, such as monitoring aggregation under crystallization conditions by scattering techniques (18). Because ribosomal particles are large enough to be detected by electron microscopy, crystals of ribosomal particles provide an excellent system for direct investigation of nucleation. The crystallization process was examined by electron microscopy. It was found that the first step in crystal growth is unspecific aggregation, and that nucleation starts by a rearrangement within the aggregates (19).

50S Ribosomal Particles from *Halobacterium marismortui*

In contrast to ribosomal particles from eubacteria, those from halobacteria are structurally stable and functionally active at high salt concentrations. Crystals from these bacteria grow under conditions which mimic, to some extent, the natural environment within the bacteria. For obtaining large and ordered crystals, advantage has been taken of the delicate equilibrium of mono- and divalent ions needed for the growth of halobacteria as well as of the major role played by the Mg^{2+}

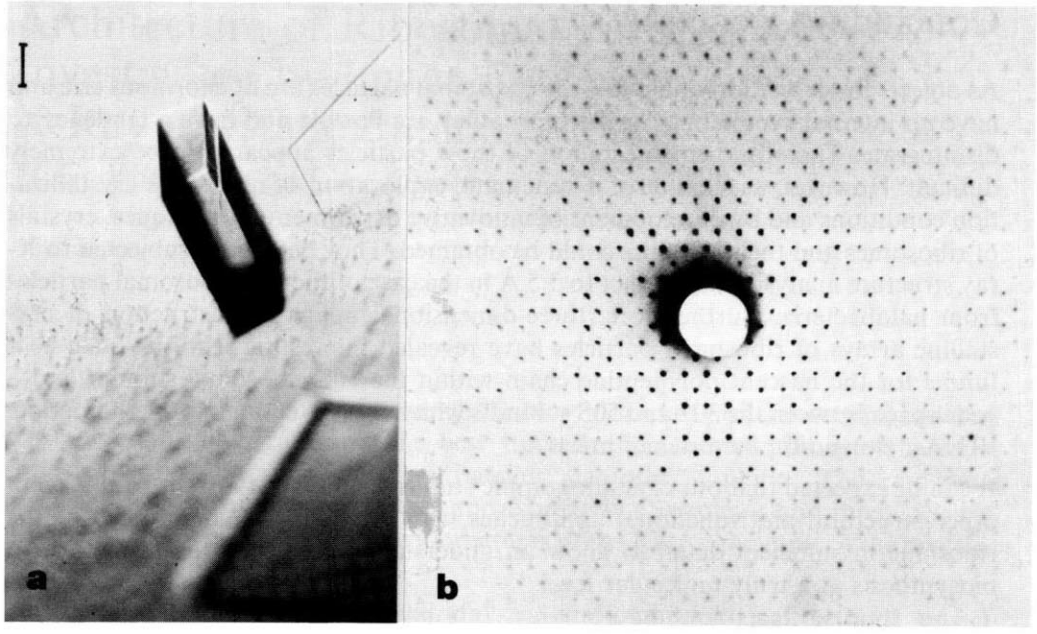

Figure 9 (a) Crystals of ribosomal 50S particles from *Halobacterium marismortui*. Bar: 0.2 mm. (b) X-ray diffraction pattern obtained at $-180\,^{\circ}C$ with synchrotron radiation.

concentration in crystallization of ribosomal particles. It was found earlier that three-dimensional crystals of 50S ribosomal subunits from *Bacillus stearothermophilus* grow in relatively low Mg^{2+} concentration, whereas the production of two-dimensional arrays requires a high Mg^{2+} concentration, at which growth of three-dimensional crystals is prohibited. Similarly, for spontaneous crystal growth of 50S subunits from *Halobacterium marismortui*, the lower the Mg^{2+} concentration is, the thicker the crystals are. With these points in mind, a variation of the standard seeding procedure has been developed. Thin crystals of the 50S subunits from *Halobacterium marismortui*, grown spontaneously under the lowest possible Mg^{2+} concentration, are transferred to mixtures in which the Mg^{2+} concentration is so low that the transferred crystals dissolve, but after several days new crystals can be observed. These are well ordered and 10–20 fold thicker than the original seeds.

Orthorhombic crystals of the 50S subunits from *Halobacterium marismortui* grow as fragile thin plates with a size of $0.6 \times 0.6 \times 0.2$ mm (Figure 9). They diffract to a resolution of 5.5 Å (15), and have relatively small and compact unit cells of $a = 214$ Å, $b = 300$ Å, $c = 590$ Å, in contrast to the open structure of the large crystals of *Bacillus stearothermophilus*. Although between $-2\,^{\circ}C$ and $4\,^{\circ}C$ up to 15 photographs can be taken from an individual crystal, the high resolution terms appear only on the first 2–3 X-ray diffraction patterns. Hence, under these conditions over 260 crystals were irradiated in order to obtain a complete data set. However, at cryo-temperature, i.e. $-180\,^{\circ}C$, irradiated crystals show hardly any radiation damage after days. Thus, for the first time, a full data set could be collected from a single crystal (unpublished results).

Concluding Remarks

As objects for crystallographic studies, ribosomal particles are of enormous size and have no internal symmetry. Furthermore, they are flexible and have a tendency to disintegrate. Therefore, crystallization of these particles appeared to be extremely difficult. However, as a result of a systematic exploration of numerous crystallization conditions and by development of innovative experimental techniques, crystals of ribosomes and their subunits could be obtained. They have been subjected to X-ray structure analysis and diffract to 5.5 Å in the case of the 50S ribosomal particles from halobacteria. Furthermore, three-dimensional image reconstruction of crystalline arrays of ribosomal particles have revealed interesting features, such as a tunnel for the nascent polypeptide chain within the 50S ribosomal subunit and a wide space between the 30S and 50S subunits which is large enough to accommodate tRNAs, elongation factors and mRNA.

It can be expected that our crystallographic studies, combined with the results from other structural and functional approaches, will eventually yield a model of the ribosome in sufficient detail to allow an understanding of the process of protein biosynthesis at a truly molecular level.

References

1. Wittmann, H.G. 1982. Ann. Rev. Biochem. *51*, 155.
2. Noller, H.F. 1984. Ann. Rev. Biochem. *53*, 119.
3. Wittmann-Liebold, B. 1986. In: Structure, Function and Genetics of Ribosomes (B. Hardesty and G. Kramer, eds). Springer, Berlin, Heidelberg, New York, p. 326.
4. Wittmann, H.G. 1983. Ann. Rev. Biochem. *52*, 35.
5. Hardesty, B. and Kramer, G. (eds.). 1986. Structure, Function and Genetics of Ribosomes. Springer, Berlin, Heidelberg, New York.
6. Yonath, A., Leonard, K.R. and Wittmann, H.G. 1987. Science *236*, 813.
7. Mathews, B.W. 1968. J. Mol. Biol. *33*, 491.
8. Malkin, L.I. and Rich, A. 1967. J. Mol. Biol. *26*, 329.
9. Blobel, B. and Sabatini, D.D. 1970. J. Cell. Biol. *45*, 130.
10. Smith, W.P., Tai, P.C. and Davis, B.D. 1978. Proc. Natl. Acad. Sci. USA *75*, 5922.
11. Barnabeau, C. and Lake, J.A. 1982. Proc. Natl. Acad. Sci. USA *79*, 3111.
12. Milligan, R.A. and Unwin, P.N.T. 1986. Nature *319*, 693.
13. Arad, T., Piefke, J., Weinstein, S., Gewitz, H.S., Yonath, A. and Wittmann, H.G. 1987. Biochemie, *69*, 1001.
14. Yonath, A., Saper, M.A., Makowski, I., Müssig, J., Piefke, J., Bartunik, H.D., Bartels, K.S. and Wittmann, H.G. 1986. J. Mol. Biol. *187*, 633.
15. Makowski, I., Frolow, F., Saper, M.A., Shoham, M., Wittmann, H.G. and Yonath, A. 1987. J. Mol. Biol. *193*, 819.
16. Yonath, A., Müssig, J. and Wittmann, H.G. 1982. J. Cell Biochem. *19*, 145.
17. Yonath, A., Leonard, K.R., Weinstein, S. and Wittmann, H.G. 1988. Cold Spring Harbor Symp., in press.
18. Kam, Z., Shore, H.B. and Fehder, G. 1978. J. Mol. Biol. *123*, 539.
19. Yonath, A., Khavitch, G., Tesche, B., Müssig, J., Lorenz, S., Erdmann, V.A. and Wittmann, H.G. 1982. Biochem. Internat. *5*, 629.